Thermal, magnetic field- and stress-induced transformation in Heusler-type Co-Cr-Al-Si shape memory alloys

doi: 10.1016/j.scriptamat.2018.04.033

Thermal, magnetic field- and stress-induced transformation in Heusler-type Co-Cr-Al-Si shape memory alloys

Takumi Odaira [a], Xiao Xu [a*], Atsushi Miyake [b], Toshihiro Omori [a], Masashi Tokunaga [b], Ryosuke Kainuma [a]

[a] Department of Materials Science, Graduate School of Engineering, Tohoku University, Aoba-yama 6-6-02, Sendai 980-8579, Japan
[b] The Institute for Solid State Physics, The University of Tokyo, Kashiwa 277-8581, Japan

Abstract

The phase diagram, including the martensitic and magnetic transformations, was determined by thermoanalysis and thermomagnetization measurements in the $Co_xCr_{79-x}Al_{10.5}Si_{10.5}$ section of the Co-based Heusler shape memory alloy. Magnetization measurements under pulsed magnetic fields were conducted and magnetic field-induced reverse martensitic transformation was clearly observed at room temperature. A superelastic behavior was obtained in the $Co_{55.7}Cr_{23.3}Al_{10.5}Si_{10.5}$ alloy in the temperature range of 198 to 423 K. The critical stress for martensitic transformation was found to show a negative temperature dependence at temperatures lower than approximately 310 K due to the magnetic effect despite the normal temperature dependence at higher temperatures.

Keywords: Co-based Heusler alloy; Shape memory alloy; Magnetic field-induced phase transition; Superelasticity; Phase diagram

Shape memory alloys (SMAs) are important functional materials because of their shape memory effect and superelasticity, and many types of SMAs have been developed, such as NiTi- [1], Ni- [2-3], Cu- [4] and Fe- [5] based alloy systems. For the last two decades, magnetic field-induced strain due to variant rearrangement [3] and magnetic field-induced reverse transformation [6] have been extensively investigated as potential magnetic actuator materials in some Heusler alloys, including Ni-Mn-X (X = In, Sn, Sb [2] and Ga [3]) alloys. Co-based Heusler alloys have attracted a great deal of attention because they present a pronounced half-metallic behavior [7-8]. Although B2-type Co-Ni-Al [9] and Co-Ni-Ga [9-11] alloys show martensitic transformation and shape memory properties, no martensitic transformations have ever been reported in Co-based Heusler alloys, expect for the case of the non-half-metallic Co_2NbSn alloy [12-13].

Recently, our research group reported new Co-Cr-Ga-Si, Co-V-Ga, Co-V-Si and Co-V-Si-Ga Heusler alloys showing martensitic transformations [14-19]. The Co-Cr-Ga-Si alloy shows unique behaviors, called reentrant martensitic transformation, where the martensite phase induced from the

paramagnetic parent phase by cooling transforms back to the ferromagnetic parent phase by further cooling. Moreover, the Co-Cr-Ga-Si alloy exhibits a cooling-induced shape memory effect, as well as a heating-induced shape memory effect, and superelasticity with inverse temperature dependence of critical stress [14]. In addition, due to the Co-Cr-Ga-Si alloy's high Cr content, it may be attractive for high corrosion-resistant biomedical SMA. However, the cost of this alloy system is relatively high because of a large amount of Ga.

Very recently, an inexpensive Co-Cr-Al-Si alloy has been found by replacing Ga with Al [20]. With crystal structures of the parent and martensite phases being $L2_1$ and $D0_{22}$, respectively, martensitic transformation and superelasticity have been confirmed in this alloy. The parent phase has also been shown to demonstrate ferromagnetic behavior and the martensite phase has been determined to be probably paramagnetic [20]. However, the martensitic transformation temperatures and Curie temperature have only been determined for two compositions, and therefore, the composition dependence of the transformation temperatures should be determined for alloy design. Moreover, neither temperature dependence of superelastic behavior nor the magnetic field-induced transformation caused by a large difference in magnetization between the parent and martensite phases have been investigated.

In this paper, we show the results of systematical research on the composition dependence of martensitic and magnetic transformations in the $Co_xCr_{79-x}Al_{10.5}Si_{10.5}$ section. Based on this knowledge, we selected suitable compositions and magnetic field-induced reverse and stress-induced forward martensitic transformations were investigated at various temperatures.

Polycrystalline $Co_xCr_{79-x}Al_{10.5}Si_{10.5}$ (Cox, x = 53.7, 54.8, 55.5, 55.7, 55.8, 55.9, 56.2, 56.3, 56.5) alloys were prepared by induction melting under an Ar atmosphere. Small pieces of samples were cut and solution-treated at 1473 K for 24 h and quenched in water. The martensitic transformation temperatures are strongly dependent on the composition and the composition analyses were conducted for each sample subjected to the following measurements, using a field emission electron probe microanalyzer with a wavelength dispersive X-ray spectrometer (FE-EPMA / WDS), and the above compositions were the analyzed one, with both the Al and Si compositions being close to 10.5 at%, as shown in Table 1. The data scattering was within ± 0.2 at%. Martensitic transformation temperatures were measured by a differential scanning calorimeter (DSC). Magnetization and thermomagnetization measurements were performed using a vibrating sample magnetometer (VSM) and a superconducting quantum interference device (SQUID) magnetometer. Magnetization measurements were also conducted using pulsed magnetic fields up to 550 kOe [21]. For the Co55.7 alloy, the cyclic heat treatment was conducted to obtain a sample with large grains by use of abnormal grain growth [22]. The pseudo-single crystal was cut out from the cyclic heat-treated ingot, sized 2.0 × 2.5 × 3.5 mm^3, with the main crystal orientation being <001>. Compression tests were performed on this Co55.7 sample from 198 to 423 K, starting from the lowest temperature. Specific

heat measurements were conducted with the heat flow method using DSC calibrated by a standard sapphire sample according to DIN 51007 at 10 K/min.

Figure 1(a) shows the results of thermoanalysis for Co55.9 and Co56.5 samples, where martensitic transformation was detected. Forward transformation starting (T_{Ms}) and finishing (T_{Mf}) temperatures and reverse transformation starting (T_{As}) and finishing (T_{Af}) temperatures are indicated. To determine these temperatures, the extrapolation method was used. While both the forward and reverse transformations were detected for the Co56.5 alloy, the peak for the forward transformation was broad and only T_{Af} was determined for the Co55.9 alloy, for which the martensite phase was partially observed at room temperature, as shown in the inset of Fig. 1(a). Thermomagnetization measurements were also carried out for another Co55.9 sample, as shown in Fig. 1(b). It has been reported that the martensite phase is paramagnetic whereas the parent phase is ferromagnetic [20], therefore the abrupt change in magnetization in Fig. 1(b) corresponds to the martensitic transformation. Note that for this sample, martensite phase was partially obtained before measurement. During 1st cooling, partial forward martensitic transformation was observed, and the transformation stopped at around 240 K denoted as T_A, and thus the sample showed still strong magnetization at temperatures below 240 K. If martensitic transformation had perfectly finished at low temperatures, the magnetization would be much weaker. This behavior is similar to the thermal transformation arrest phenomenon, as reported in NiMn-based alloys [23-24]. At the arrest temperature (T_A), the transformation entropy change (ΔS) has been reported to be zero, therefore the forward martensitic transformation does not occur below this temperature anymore, which is defined as the temperature where both heating and cooling thermomagnetization curves overlap [23-24]. After 1st cooling, the samples were then heated to 390 K to obtain full parent phase, and the T_{Ms} were determined from 2nd cooling curve. For Co55.9 in Fig 1(a), since the parent phase is considered to partially exist after cooling, therefore, strictly speaking, T_{As} of Co55.9 in Fig. 1(a) is not the starting temperature of the reverse martensitic transformation. Figure 1(c) shows the thermomagnetization curves under a magnetic field of 5 kOe, where the Curie temperature (T_C) of the parent phase was defined as the temperature with a maximum gradient. Here, the thrmonagnetization curve of Co55.9 in Fig. 1(c) is obviously different from that in Fig. 1(b), which is caused by macroscopic inhomogeneity in distribution of martensite phase in Co55.9 sample.These martensitic and magnetic transformation temperatures are listed in Table 1 with their compositions and plotted against Co content in Fig. 1(d), where T_0 (= (T_{Ms} + T_{Af})/2) is assumed to be the thermodynamic equilibrium temperature. Note that for Co55.9, samples including large amount of martensite phase were used for detecting martensitic transformation temperatures (Fig. 1(a) and (b)) and a sample with small amount of that was used for detecting the Curie temperature (Fig. 1(c)), which is indicated by an asterisk in Table 1 aside the alloy's name. The transformation temperatures determined by thermomagnetization measurements are shown with daggers, otherwise by

thermoanalysis. It can be seen in Fig. 1(d), the Curie temperature slightly decreases while the martensitic transformation temperatures drastically increase with increasing Co concentration. Interestingly, the martensitic transformation is strongly suppressed when the parent phase is ferromagnetic due to the magnetic effect [15], and martensitic transformation could not be obtained for $x < 55.8$ alloys. The possibility of reentrant martensitic transformation shown in the circle in Fig. 1(b) and as broken lines for T_{Ms} and T_0 in Fig. 1(d) will be discussed later. The martensitic transformation is influenced by aging [20], therefore, the transformation temperatures were difficult to be determined in the higher temperature region.

Figure 2(a) shows the results of magnetization curves measured at 6 K for the Co53.7 and Co55.8 samples. Ferromagnetic behavior was observed for Co53.7, and this sample was considered to have an almost full parent phase, because its spontaneous magnetization was found to be 68 emu/g, which is approximately the same as that of a full-parent-phase sample with a close composition of $Co_{55}Cr_{23}Al_{11}Si_{11}$ [20]. One of the Co55.8 samples, denoted as Co55.8H, shows higher magnetization while the other (Co55.8L) has much lower magnetization. Because the martensite phase is paramagnetic [20], the Co55.8 samples are considered to partially have the martensite phase, and the volume fraction of the martensite phase is much larger in Co55.8L, although they were obtained from the same ingot and neither obvious composition difference nor inhomogeneity was found through chemical composition analysis by use of EPMA. A pulsed magnetic field up to 550 kOe was applied to the Co55.8L sample at 300 K and the result is shown in Fig. 2(b). Large hysteresis was observed, which was due to the magnetic field-induced reverse martensitic transformation and the reverse transformation during the removal of the magnetic field. Because the magnetization of the parent phase is greater than that of martensitic phase, a magnetic field can stabilize the parent phase, as observed in the Ni-based Heusler alloys [6, 25]. The reverse martensitic transformation in Fig. 2(b) does not seem to finish even though the magnetic field was as strong as 550 kOe, and only partial phase transition was observed. This is the first time that the magnetic field-induced reverse transformation in the Co-based Heusler alloys has been obtained, implying the magnetic field-induced shape memory effect.

As shown in Fig. 1(c), since no thermal martensitic transformation was obtained for Co55.7, uniaxial compression tests were performed at various temperatures on this sample, with an expectation of stress-induced forward martensitic transformation. The results of compression tests on the Co55.7 sample are shown in Fig. 3(a). Superelasticity was obtained in a wide temperature range from 198 to 423 K. The forward martensitic transformation starting stress (σ_{Ms}) and reverse martensitic transformation finishing stress (σ_{Af}) were defined by the extrapolation method, as indicated in Fig. 3(a). The critical stresses in Fig. 3(a) are plotted against temperature in Fig. 3(b), where $\sigma_0 = (\sigma_{Ms} + \sigma_{Af})/2$ is assumed to be the thermodynamic equilibrium stress. At temperatures higher than 310 K, critical stress increases with increasing testing temperature, which is the same as

conventional SMAs, such as Ni-Ti [26] and Cu-Al-Mn [27]. At lower temperatures, however, an inverse temperature dependence of critical stress was observed. A similar anomaly has been reported in Co-Cr-Ga-Si [14, 16]. In the compression test conducted at 423 K, the superelastic loop shows a different shape with larger hysteresis compared with those of other temperatures. The critical stresses at 423 K also showed large deviation. This may originate from the aging effect [20]; therefore the results for this temperature were excluded from the following thermodynamic discussion.

The Clausius-Clapeyron equation for uniaxial stress can be written as

$$\frac{\mathrm{d}\sigma_0}{\mathrm{d}T} = -\frac{\Delta S}{\varepsilon V}$$

where ε, V and $\Delta S = S_M - S_P$ are the transformation strain, molar volume and entropy change during martensitic transformation, respectively. Here, the transformation strain of this sample was assumed to be that for the <001> crystal orientation because this sample is a pseudo-single crystal with a main orientation of <001> and the critical stress of <001> is the lowest. Each value of $\mathrm{d}\sigma_0/\mathrm{d}T$ was estimated by the inclination between adjacent measured values. The lattice parameters of the parent and martensite phases obtained in previous research [20] were used for calculating transformation strain (ε = 6.05%) and atomic molar volume ($V = 6.93 \times 10^{-6}$ m^3/mol). In addition, the ΔS during martensitic transformation was obtained from specific heat measurements by DSC for two samples of Co56.5 (shown by Sample 1, 2 in Fig. 4(b)), with one of the heating processes being shown in Fig. 4(a). ΔS from 198 K to 398 K calculated by the Clausius–Clapeyron equation using the experimental result of temperature dependence of critical stress, and two sets of ΔS measured by DSC during both heating and cooling, are plotted in Fig. 4(b). It can be seen from Fig. 4(b) that ΔS becomes zero at approximately 310 K (shown as T'_A in Fig. 4(b)), which is slightly lower than the Curie temperature, and ΔS shows negative values above this temperature, whereas positive ones are evident below this temperature. The reason for this abnormal sign reversal behavior of ΔS has been considered to be the change of magnetic entropy of the parent phase below the Curie temperature, which is a similar behavior to that in Co-Cr-Ga-Si alloys [15, 16], except for the fact that the sign reversion temperature T'_A for Co55.7 is much lower than that of Co-Cr-Ga-Si alloys ($T_A \approx 500$ K) [16].

In the binary Ni-Ti system, the shape of the σ_0-T curve has been shown to be similar to that of the temperature-composition T_0-x curve, and therefore $\mathrm{d}x / \mathrm{d}T_0$ becomes infinity at the same temperature where $\mathrm{d}\sigma_0 / \mathrm{d}T$ and ΔS are zero [28]. However, the T_A determined by the thermomagnetization measurements is about 230 K, which is much lower than T'_A estimated from the compression tests, which is about 310 K. The difference between T_A and T'_A may partially originate from the fact that the T_C shows obvious Co-composition dependence, which has been pointed out for the cases of Co-Cr-Ga-Si alloys [16]. Therefore, we expect the gradient of the T_0 curve in Fig. 1(d) should become infinity at approximately 240 K shown by T_A in Fig. 1(d), where ΔS becomes zero.

Generally, the driving force during thermal transformation can be roughly estimated as $\Delta G = \Delta S \cdot \Delta T$. Thus, the drastic change in transformation temperatures in Fig. 1(d) can be understood because the driving force for martensitic transformation becomes zero at approximately 240 K; therefore no forward martensitic transformation can be observed below this temperature. Furthermore, a change of sign of ΔS can be expected below T_A. Therefore, below T_A, the driving force also shows an opposite sign and the parent phase becomes more favorable when the temperature is lower. This results in an expectation of curvatures of the composition dependence of martensitic transformation temperatures and the martensite phase may form a "martensite loop", as shown by the broken lines in Fig. 1(d). The reentrant martensitic transformation behavior should occur if a martensite phase sample could pass through the T_{As} temperature. As shown in Fig. 1(b), at around 150 K for Co55.9, a small hysteresis loop was observed from the thermomagnetization curves. However, it is still not confidential to conclude this is the experimental evidence of reentrant martensitic transformation in the Co-Cr-Al-Si system. Further investigations are required to clarify this point.

In summary, the martensitic and magnetic transformation temperatures were determined for $Co_xCr_{79-x}Al_{10.5}Si_{10.5}$ Heusler alloys. The martensitic transformation could be observed in alloys with higher Co compositions in the paramagnetic range, but for those with lower Co compositions in the ferromagnetic state of the parent phase ($x < Co55.8$), thermal martensitic transformation was not observed. For a two-phase (martensite + parent) sample, magnetic field-induced reverse partial martensitic transformation was observed by magnetization measurement under a pulsed high magnetic field. Superelasticity was obtained in a wide temperature range between 198 K and 423 K, and the critical stress showed parabolic-like behavior against temperature. This was due to an evolution of transformation entropy change (ΔS) from negative to positive values caused by the magnetic effect of the parent phase and ΔS becomes zero at around room temperature. This thermodynamic property results in the absence of driving force for thermal martensitic transformation, which leads to the drastic change of martensitic transformation temperature against Co composition.

Acknowledgements

A part of the experiments was performed at the Center for Low Temperature Science, Institute for Materials Research, Tohoku University. This study was supported by JSPS KAKENHI Grand Numbers 15H05766 and 16H06632.

References

1. W. J. Buehler, J.V. Gilfrich, R. C. Wiley, J. Appl. Phys. 34 1475 (1963)
2. Y. Sutou, Y. Imano, N. Koeda, T. Omori, R. Kainuma, K. Ishida, K. Oikawa, Appl. Phys. Lett. 85 4358 (2004)

3. Ullakko, J.K. Huang, C. Kantner, R.C. O'Handley, V.V. Kokorin, Appl. Phys. Lett. 69 1966-1968 (1996)
4. R. Kainuma, S. Takahashi, K. Ishida, Metall. Mater. Trans. A 27 2187 (1996)
5. T. Omori, K. Ando, M. Okano, X. Xu, Y. Tanaka, I. Ohnuma, R. Kainuma, K. Ishida, Science 333 68-71 (2011)
6. R. Kainuma, Y. Imano, W. Ito, Y Sutou, H. Morito, S. Okamoto, O. Kitakami, K. Oikawa, A. Fujita, T. Kanomata, K. Ishida, Nature 439 957-960 (2006)
7. A. Kellou, N. E. Fenineche, T. Grosdidier, H. Aourag, C. Coddet, J. Appl. Phys. 94 3292-3298 (2003)
8. R. Y. Umetsu, A. Okubo, X. Xu, R. Kainuma, J. Alloys Compd. 588 153-157 (2014)
9. K. Oikawa, T. Ota, F. Gejima, T. Omori, R. Kainuma, K. Ishida, Mater. Trans. 42 2472 (2001)
10. M. Wutting, J. Li, C. Craciunescu, Scripta Mater. 44 2393-2397 (2001)
11. J. Dadda, H. J. Maier, I. Karaman, H. E. Karaca, Y. I. Chumlyakov, Scripta Mater. 55 663-666 (2006)
12. M. Terada, Y. Fujita, K. Endo, J. Phys. Soc. Jpn. 36 620 (1974)
13. S. Fujii, S. Ishida, S. Asano, J. Phys. Soc. Jpn. 58 3657-3665 (1989)
14. X. Xu, T. Omori, M. Nagasako, A. Okubo, R. Umetsu, T. Kanomata, K. Ishida, R. Kainuma, Appl. Phys. Lett. 103 164104 (2013)
15. X. Xu, M. Nagasako, M. Kataoka, R. Umetsu, T. Omori, T. Kanomata, R. Kainuma, Phys. Rev. B 91 104434 (2015)
16. X. Xu, T. Omori, M. Nagasako, T. Kanomata, R. Kainuma, Appl. Phys. Lett. 107 181904 (2015)
17. X. Xu, A. Nagashima, M. Nagasako, T. Omori, T. Kanomata, R. Kainuma, Appl. Phys. Lett. 110 121906 (2017)
18. H. Jiang, X. Xu, T. Omori, M. Nagasako, J. Ruan, S. Yang, C. Wang, X. Liu, R. Kainuma, Mater. Sci. Eng. A 676 191-196 (2016)
19. H. Jiang, C. Wang, W. Xu, X. Xu, S. Yang, R. Kainuma, X. Liu, Mater. Design 116 300-308 (2017)
20. K. Hirata, X. Xu, T. Omori, M. Nagasako, R. Kainuma, J. Alloys Compd. 642 200-203 (2015)
21. K. Kindo, Physica B 294-295 588-590 (2001)
22. T. Omori, T. Kusama, S. Kawata, I. Ohnuma, Y. Sutou, Y. Araki, K. Ishida, R. Kainuma, Science 341 6153 1500-1502 (2013)
23. W. Ito, K. Ito, R. Y. Umetsu, R. Kainuma, K. Koyama, K. Watanabe, A. Fujita, K. Oikawa, K. Ishida, T. Kanomata, Appl. Phys. Lett. 92 021908 (2008)
24. X. Xu, W. Ito, M. Tokunaga, T. Kihara, K. Oka, R. Y. Umetsu, T. Kanomata, R. Kainuma, Metals 3 298-311 (2013)
25. R. Kainuma, Y. Imano, W. Ito, H. Morito, Y. Sutou, K. Oikawa, A. Fujita, K. Ishida, S.

Okamoto, O. Kitakami, T. Kanomata, Appl. Phys. Lett. 88 192513 (2006)
26. S. Miyazaki, K. Otsuka, Y. Suzuki, Scripta Metall. Mater. 15 287-292 (1981)
27. K. Niitsu, T. Omori, R. Kainuma, Mater. Trans. 52 8 1713-1715 (2011)
28. K. Niitsu, Y. Kimura, X. Xu, R. Kainuma, Shap. Mem. Superelasticity 1:124-131 (2015)

Table 1. Composition, phase observed at room temperature, Curie temperature of parent phase T_C, forward martensitic transformation starting (T_{Ms}) and finishing (T_{Mf}) temperatures and reverse martensitic transformation starting (T_{As}) and finishing (T_{Af}) temperatures of $Co_xCr_{79-x}Al_{10.5}Si_{10.5}$ (Cox) alloys. The transformation temperatures determined by thermomagnetization measurements are shown with daggers, otherwise by thermoanalysis. For Co55.9, the asterisk aside the composition indicates that measurements were conducted on different samples for these alloys. Refer to the text for details.

	Composition %				Phase	Transformation temperature (K)				
Alloy	Co	Cr	Al	Si		T_{As}	T_{Af}	T_{Ms}	T_{Mf}	T_C
Co53.7	53.7	25.8	10.1	10.4	P	-	-	-	-	393†
Co54.8	54.8	24.5	10.2	10.5	P+M	-	-	-	-	387†
Co55.5	55.5	23.9	10.1	10.5	P+M	-	-	-	-	370†
Co55.7	55.7	23.7	10.4	10.2	P	-	-	-	-	377†
Co55.8	55.8	23.7	10.1	10.4	P+M	-	-	-	-	367†
Co55.9*	55.9	23.4	10.4	10.3	P+M	-	364 / 375†	- / 337†	-	361†
Co56.2	56.2	23.1	10.4	10.3	P+M+γ	349	383	350	294	-
Co56.3	56.3	22.7	10.4	10.6	M+γ	370	404	369	324	-
Co56.5	56.5	22.6	10.5	10.4	M+γ	364	397	376	329	-

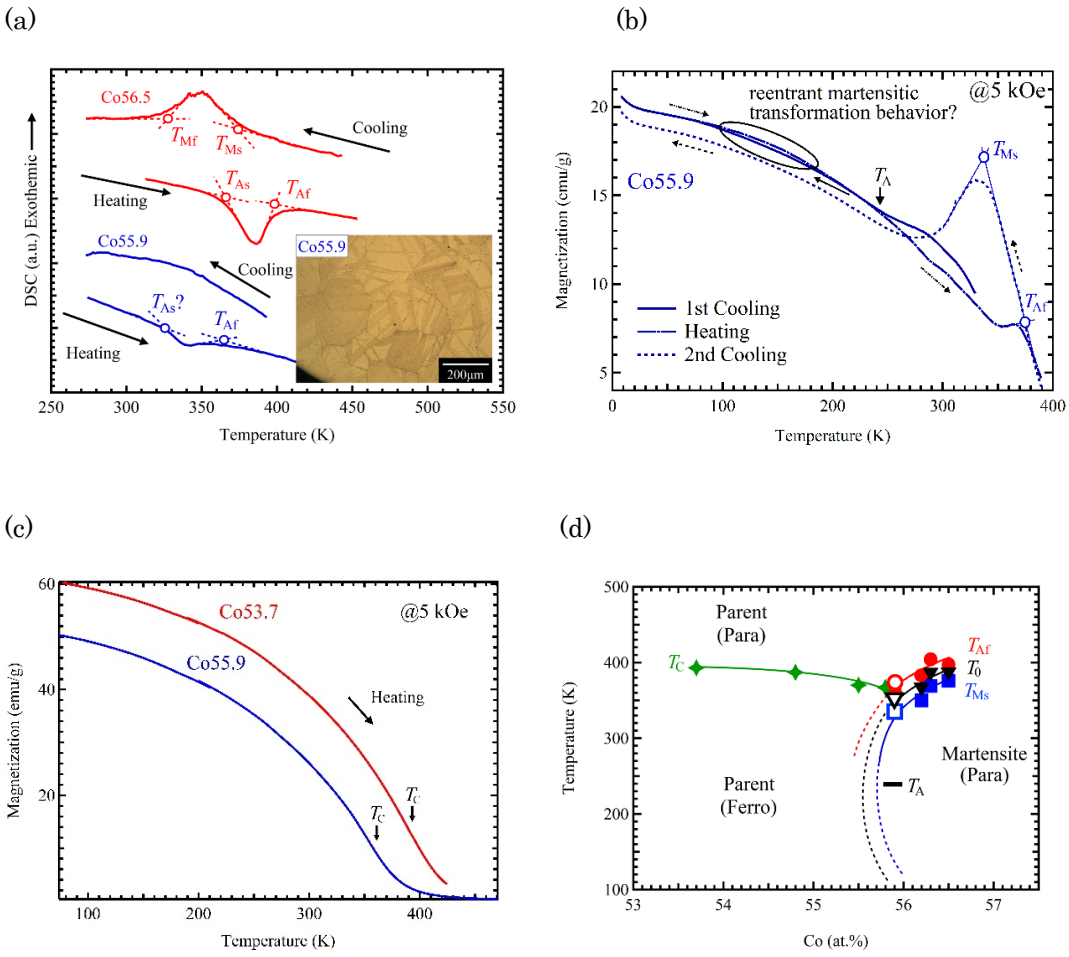

FIG. 1. Results of (a) thermoanalysis and (b) and (c) thermomagnetization measurements under 5 kOe for Co53.7, Co55.9 and Co56.5 samples. In (a), martensitic transformation temperatures are determined. In addition, the martensite phase partially observed for Co55.9 at room temperature is also shown in the inset. (b) Martensitic transformation temperatures and thermal transformation arrest temperature (T_A) are shown for Co55.9. In (c), Curie temperature (T_C) is defined as the temperature with a maximum gradient. These temperatures are plotted in (d) the magnetic phase diagram for $Co_xCr_{79-x}Al_{10.5}Si_{10.5}$ alloys, where $T_0 = (T_{Ms} + T_{Af})/2$). In (d), T_{Af}, T_0 and T_{Ms} determined from (a) and (c) are shown as closed and open marks, respectively. Curie temperature slightly decreases and martensitic transformation temperatures strongly increase with increasing Co concentration.

(a)

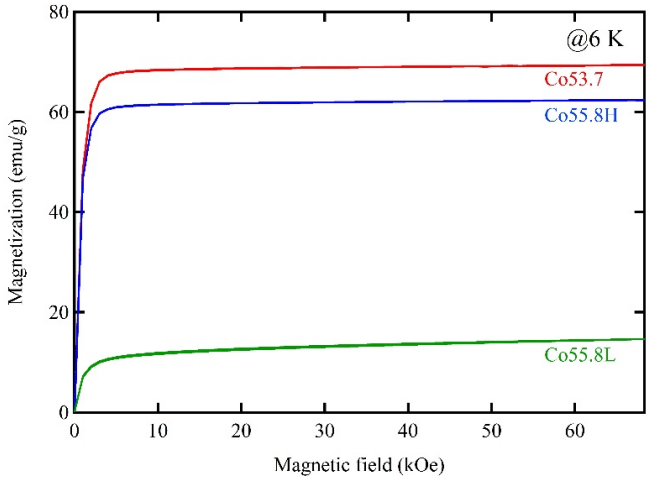

(b)

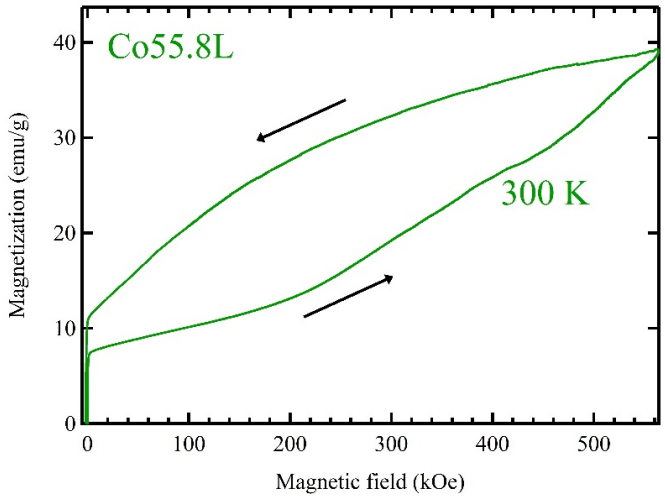

FIG. 2. Magnetization curves measured for (a) Co53.7 and Co55.8 at 6 K and (b) Co55.8L under a pulsed high magnetic field at 300 K. For (a), while ferromagnetic behaviors were observed for all samples, their values of spontaneous magnetization were different due to the different amount of residual parent phase. For (b), magnetic field-induced reverse martensitic transformation was observed.

(a)

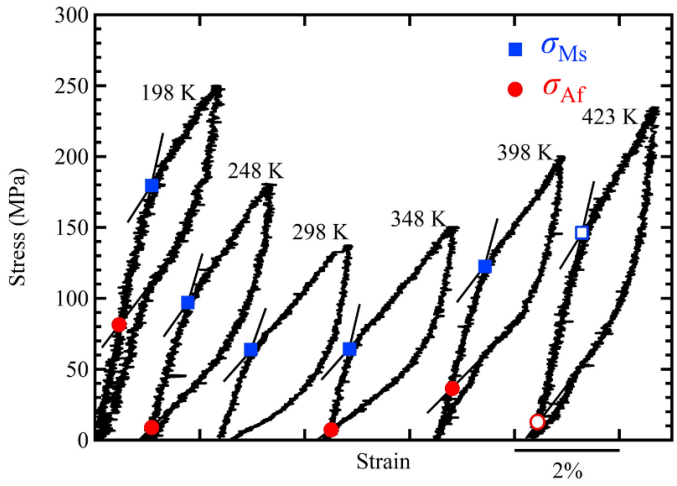

(b)

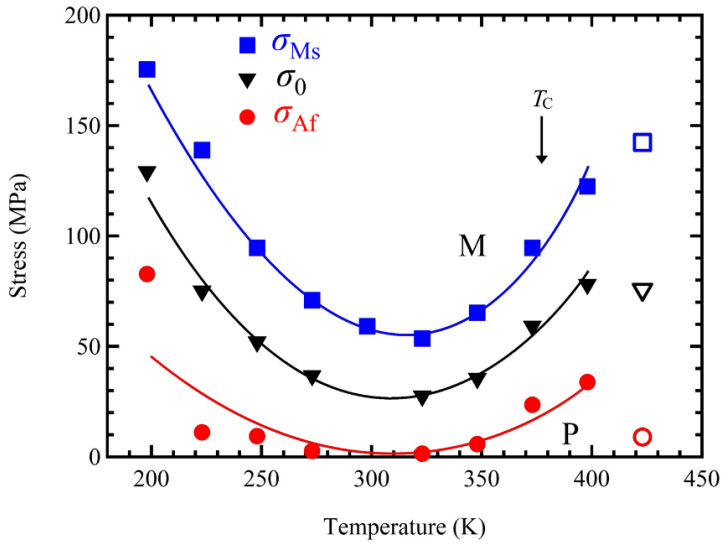

FIG. 3. (a) Compression tests for a Co55.7 alloy from 198 to 423 K. The forward martensitic transformation starting stress (σ_{Ms}) and reverse martensitic transformation finishing stress (σ_{Af}) were defined by the extrapolation method, as indicated in (a). (b) σ_{Ms}, σ_{Af} and $\sigma_0 = (\sigma_{Ms} + \sigma_{Af})/2$ are plotted.

(a)

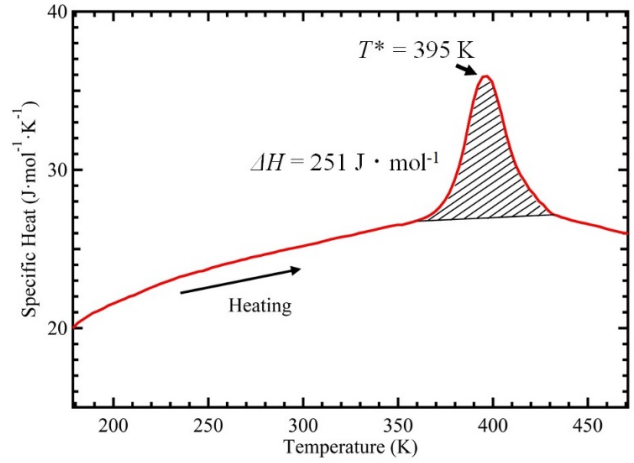

(b)

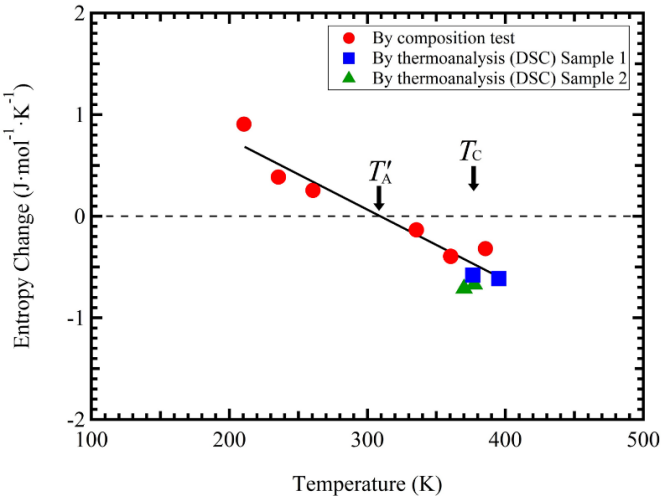

FIG.4 (a) The result of specific heat measurement with the heat flow method during the heating process. The transformation enthalpy change during the reverse martensitic transformation ΔH was determined by estimating the hatched area and the peak temperature (T*) was measured for Co56.5. (b) The entropy change during the martensitic transformation ($\Delta S = S_M - S_P$) is estimated by thermoanalysis and by using the Clausius–Clapeyron relationship. ΔS becomes zero at approximately 310 K (shown as T'_A) and reversal of the sign of entropy change is expected.